# First and Second Sound in a Compressible 3D Bose Fluid

Timon A. Hilker,[1,*,†] Lena H. Dogra,[1] Christoph Eigen,[1] Jake A. P. Glidden,[1] Robert P. Smith,[2] and Zoran Hadzibabic[1]

[1]Cavendish Laboratory, University of Cambridge, J. J. Thomson Avenue, Cambridge CB3 0HE, United Kingdom
[2]Clarendon Laboratory, University of Oxford, Parks Road, Oxford OX1 3PU, United Kingdom

(Received 31 December 2021; accepted 12 April 2022; published 2 June 2022)

The two-fluid model is fundamental for the description of superfluidity. In the nearly incompressible liquid regime, it successfully describes first and second sound, corresponding, respectively, to density and entropy waves, in both liquid helium and unitary Fermi gases. Here, we study the two sounds in the opposite regime of a highly compressible fluid, using an ultracold $^{39}$K Bose gas in a three-dimensional box trap. We excite the longest-wavelength mode of our homogeneous gas, and observe two distinct resonant oscillations below the critical temperature, of which only one persists above it. In a microscopic mode-structure analysis, we find agreement with the hydrodynamic theory, where first and second sound involve density oscillations dominated by, respectively, thermal and condensed atoms. Varying the interaction strength, we explore the crossover from hydrodynamic to collisionless behavior in a normal gas.

DOI: 10.1103/PhysRevLett.128.223601

One of the hallmarks of superfluidity is the existence of two distinct sound modes with the same wavelength, corresponding to two different sound speeds. This remarkable property is the key prediction of the hydrodynamic two-fluid model, which was conceptualized by Tisza [1] and London [2], and established by Landau using quantum hydrodynamics [3,4]. In this model, the two fluids are the superfluid and the normal component of a system below its critical temperature $T_c$. Originally inspired by superfluid $^4$He, Landau's theory successfully predicts properties of this strongly interacting, essentially incompressible fluid. More recently, two sound modes have been observed in ultracold atomic Fermi gases near unitarity [5–7], which are also nearly incompressible.

Ultracold Bose gases provide a versatile platform to test the same general framework for highly compressible superfluids, including the hybridization of the two modes [8] [see Fig. 1(a)]. However, a challenge in these systems is reaching hydrodynamic conditions for the normal fluid, which requires the collisional mean free path $\ell_{\rm mfp}$ to be significantly shorter than the excitation wavelength. In harmonically trapped gases, following first studies of collisionless excitations [9–11], a pioneering study [12] revealed the analogs of first and second sound in two collective modes with frequencies between the hydrodynamic and collisionless predictions. Further studies have explored the effects of interactions on the first sound above $T_c$ [13,14] and on the second sound and related thermodynamics below it [15–17]. Recently, simultaneous observation of first and second sound has been used to characterize the superfluid transition in two dimensions (2D) [18].

Here, we realize the compressible-fluid regime of the two-fluid model in the textbook setting of a 3D homogeneous Bose gas, using tuneable interactions between $^{39}$K atoms to attain hydrodynamic conditions. Below $T_c$, we observe both first and second sound, with speeds in agreement with Landau's theory. Using momentum-resolved measurements, which give access to the motion of the spatially overlapping superfluid and normal components, we reveal the structure of the two sound modes. For gases above $T_c$, where only the first sound remains, we also investigate the effects of viscous damping by reducing the interaction strength and crossing from the hydrodynamic to the collisionless regime.

In the hydrodynamic two-fluid model, the superfluid and normal components are characterized by their densities

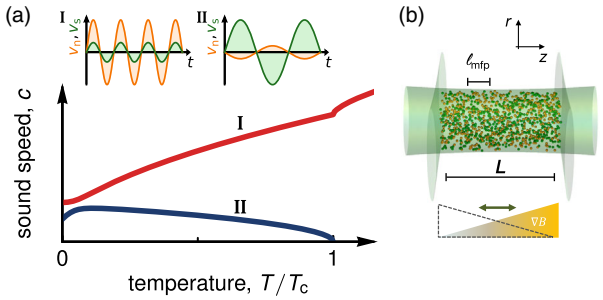


FIG. 1. First and second sound in dilute Bose gases. (a) Mode structure and speeds of sound in a weakly interacting Bose gas based on the two-fluid model. Both modes involve motion of both fluids ($v_s$, $v_n$), but for $k_B T \gg g n_s$, where $g$ is the interaction strength and the first (second) sound is mainly an oscillation of the normal (superfluid) component. (b) In a box-trapped gas of $^{39}$K atoms, we excite the $k_L = \pi/L$ mode of both sounds by sinusoidal forcing using a magnetic gradient $\nabla B$. To attain hydrodynamic conditions, we reduce the mean free path $\ell_{\rm mfp}$ below the box length $L$ by tuning $g$.

 

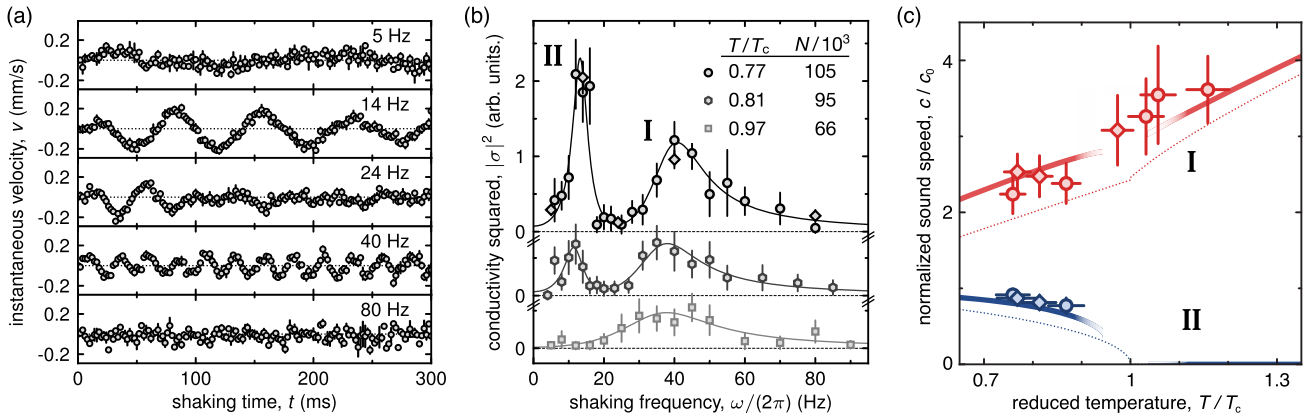


FIG. 2. Observation of first and second sound. (a) Center-of-mass velocity $v$ versus shaking time $t$ at several frequencies $\omega/(2\pi)$ reaching quasisteady state after 200 ms. (b) $|\sigma(\omega)|^2$, where $|\sigma(\omega)|$ is proportional to the amplitude of the total current $Nv(t)$. The two peaks correspond to the two sound modes. We show spectra for different $N$ at approximately constant $T = 97(3)$ nK (measured at $t = 200$ ms). The solid lines are fits using the sum of two resonances [20]. The diamonds correspond to the data shown in (a). (c) First (red) and second (blue) sound speeds, normalized by the Bogoliubov speed $c_0(N)$, versus $T/T_c$. The diamonds correspond to data shown in (b). The solid lines are the fit-free predictions of the two-fluid model [Eq. (2)] at fixed $T = 97$ nK and varying $N$, with $n_s$ calculated using Popov mean-field theory. Near $T_c$ mean-field theory is not valid, which we represent by fading of the lines. The dotted lines show $c_{\mathrm{I}}$ of a noninteracting gas and $c_{\mathrm{II}}$ calculated by equating $n_s$ with condensate density $n_{\mathrm{BEC}}$, and calculating $n_{\mathrm{BEC}}$ in the ideal-gas approximation.

$(n_s, n_n)$ and velocities $(v_s, v_n)$. In the nearly incompressible liquid helium, the first sound is an in-phase oscillation of the two coupled components, while the second sound is an out-of-phase oscillation that corresponds to a pure temperature or entropy per particle wave $\delta\tilde{s} \propto v_n - v_s$. On the other hand, in a strongly compressible gas the two components largely decouple. As illustrated in Fig. 1(a), in this regime the first and second sound, respectively, are predominantly $v_n$ and $v_s$ modes [8,19].

Generally (see the Supplemental Material [20] for details), one can write an eigenvalue equation [3,34] for the sound speed $c$ in the basis of total density $n = n_n + n_s$ and entropy per particle $\tilde{s}$:

$$b^2 \begin{pmatrix} J^2/K^2 & J \\ J & 1 \end{pmatrix} \begin{pmatrix} \frac{\delta n}{n} \\ \frac{\delta\tilde{s}}{\tilde{s}} \end{pmatrix} = c^2 \begin{pmatrix} 1 & 0 \\ 0 & \frac{n_n}{n_s} \end{pmatrix} \begin{pmatrix} \frac{\delta n}{n} \\ \frac{\delta\tilde{s}}{\tilde{s}} \end{pmatrix}, \quad (1)$$

where $K^2 \equiv (1 - c_V/c_P)$ [35], $J \equiv -(n/\tilde{s})[(\partial\tilde{s})/(\partial n)]_{T,V}$, and $b^2 \equiv nT\tilde{s}^2/(mc_V)$, with heat capacities $c_{V,P}$ per volume $V$, temperature $T$, and atom mass $m$. For an incompressible gas, $K \to 0$ and $J \sim 1$ for any $T < T_c$, so the two modes are oscillations of $n$ and $\tilde{s}$ [8]. In the opposite, ideal-gas limit [37], $K, J \to 1$, the $n$ and $\tilde{s}$ modes maximally hybridize; here the eigenmodes correspond to motion of either the normal or the superfluid component. In general, the crossover between the two regimes is primarily controlled by the value of $K$, which can vary between zero and one.

In a weakly interacting Bose gas, where thermodynamic quantities can be calculated from first principles, $K$ changes smoothly from zero to almost one as the temperature is varied from zero to $T_c$ [8]. Here we explore the compressible regime, $k_B T \gg gn$, where $g = 4\pi\hbar^2 a/m$ and $a$ is the $s$-wave scattering length. In Hartree–Fock mean-field theory, $K = 1 - gn^2/[2\chi(z)n_n k_B T]$ and the sound speeds are [20,38]

$$c_{\mathrm{I}}^{(\mathrm{HF})} = \sqrt{\chi(z)\frac{k_B T}{m} + 2\frac{gn_n}{m}}, \qquad c_{\mathrm{II}}^{(\mathrm{HF})} = \sqrt{\frac{gn_s}{m}}, \quad (2)$$

where $\chi(z) = 5g_{5/2}(z)/[3g_{3/2}(z)]$, $g_\alpha(z)$ are polylogarithms, and $z = e^{\mu^*/(k_B T)}$ is evaluated using $\mu^* = -gn_s$ below $T_c$ [39]. While $c_{\mathrm{II}}^{(\mathrm{HF})}$ depends strongly on interactions, $c_{\mathrm{I}}^{(\mathrm{HF})}$ is to leading order set by just the temperature.

Our experiments start with a partially condensed Bose gas of $^{39}$K atoms in the lowest hyperfine state, confined in a cylindrical box trap [40–42] of length $L = 70(2)$ $\mu$m and radius $R = 9.2(5)$ $\mu$m. To create hydrodynamic conditions we tune $a$ to a relatively high 480(20) $a_0$ using the magnetic Feshbach resonance at 402.7 G [43]. This enhances three-body losses and heating, but within 200 ms the gas reaches a trap-depth–limited $T = 97(3)$ nK (see the Supplemental Material [20]), at which point the atom number is $N = 105(3) \times 10^3$, corresponding to $T/T_c = 0.77(3)$ [44], $\ell_{\mathrm{mfp}} = (8\pi n a^2)^{-1} = 0.15(1)L$, $K = 0.75(5)$, $J = 1.20(4)$, and $b = 3.2(2)$ mm s$^{-1}$.

After tuning $a$, we start weakly exciting the lowest sound mode(s), with wave vector $k_L = \pi/L$, using a spatially uniform force of magnitude $F = F_0 \sin(\omega t)$, with $F_0 L/k_B = 7.7$ nK [45], generated by an axial magnetic gradient [46]. After a variable time $t$, we turn off both $F$ and the trap, and measure the axial 1D momentum distribution

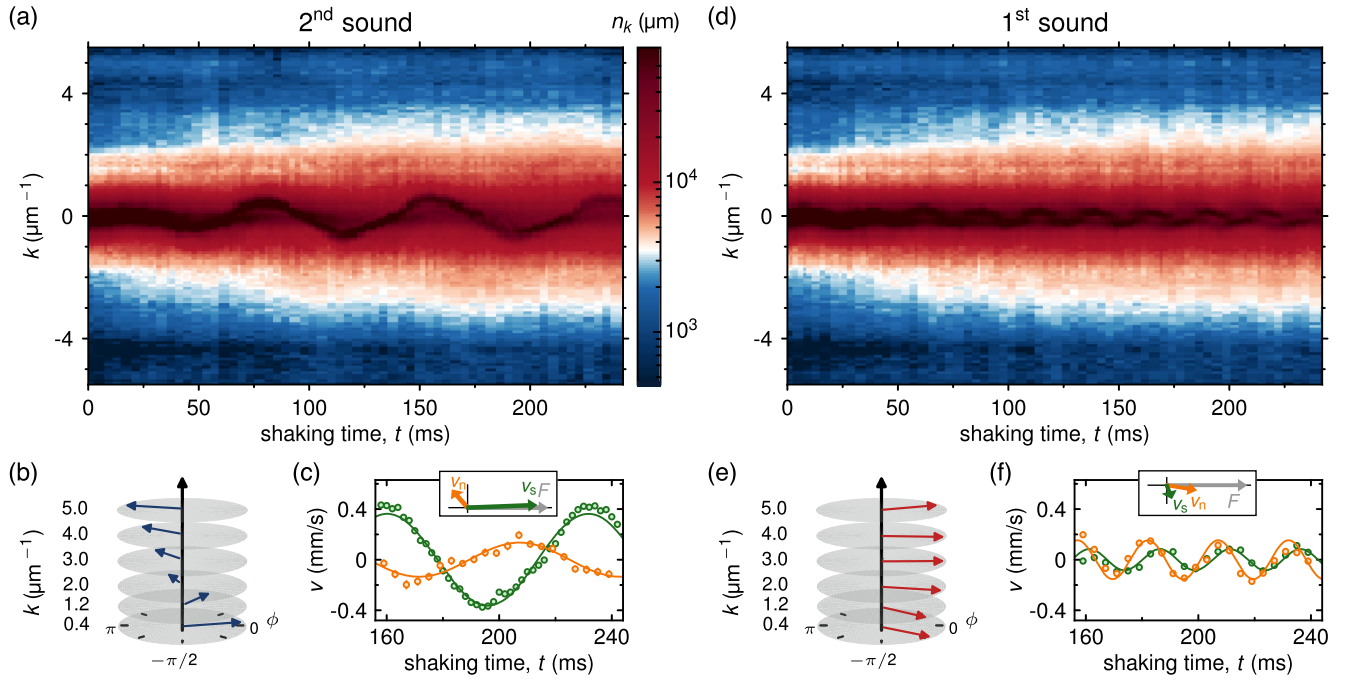


FIG. 3. Microscopic structure of the two sound modes. Here $T/T_c = 0.77(3)$, corresponding to a superfluid fraction of 43(3)%. (a) Evolution of $n_k$ on the second-sound resonance at 14 Hz [see Fig. 2(b)]. The motion of the superfluid at low $k$ is visually clear, and from the wings of the distribution one can also extract the normal-gas velocity $v_n$. (b) $k$-resolved phase $\phi$ (with respect to the phase of the drive) of the $n_k(t)$ oscillations. Here the low- and high-$k$ oscillations are almost completely out of phase, as predicted for second sound. (c) Extracted $v_n$ (orange) and $v_s$ (green); $v_s$ is larger and in phase with the drive (see phasor in the inset) as expected for a compressible superfluid. (d)–(f) Analogous analysis to (a)–(c), now for the first-sound resonance at 40 Hz; here $\phi$ is close to 0 for all $k$ and $v_n$ is larger than $v_s$.

$n_k(t)$ using a time-of-flight expansion of 30–45 ms. The cloud's center-of-mass (COM) velocity $v(t) = \hbar\langle k\rangle/m$, shown in Fig. 2(a) for various $\omega$, gives the current density due to both components, $j = nv = n_s v_s + n_n v_n$. This provides a model-free description of the system response, which we characterize in (quasi-) steady state ($t \gtrsim 200$ ms) using the analog of a complex optical (nonzero-frequency) conductivity $\sigma \propto j/F$ [47].

In Fig. 2(b) (top curve) we plot the full spectrum $|\sigma(\omega)|^2$ at $T/T_c = 0.77$, which reveals two well-resolved peaks corresponding to the two sound modes. In our homogeneous system, the resonance frequencies $\omega_{\mathrm{I}}$ and $\omega_{\mathrm{II}}$ directly give the speeds $c_{\mathrm{I,II}} = \omega_{\mathrm{I,II}}/k_L$. To study sound modes at higher $T/T_c$, we lower $N$ at approximately fixed $T$ [20]. We see that the response at $\omega_{\mathrm{II}}$ weakens and vanishes, while the response at $\omega_{\mathrm{I}}$ persists [lower curves of Fig. 2(b)].

In Fig. 2(c) we summarize our measurements of $c_{\mathrm{I,II}}$ for various $T/T_c$ below and above 1. Here, we normalize the speeds by the Bogoliubov speed $c_0 = [gN/(\pi R^2 Lm)]^{1/2}$. We find good agreement with the predictions of Eq. (2) without any free parameters (solid lines), with $n_s$ calculated within the mean-field Popov approximation [20]. For reference, we also show the ideal-gas prediction for $c_{\mathrm{I}}$ [48] and the prediction for $c_{\mathrm{II}}$ assuming that $n_s = n_{\mathrm{BEC}}$, and calculating $n_{\mathrm{BEC}}$ in the ideal-gas approximation.

We next explore the $k$-space structure of the two sound modes, focusing on our $T/T_c = 0.77$ dataset, for which the superfluid fraction is 43(3)%. Figures 3(a) and 3(d) show the time evolution of the axial $n_k$ distribution for shaking near the second- and first-sound resonance (at 14 and 40 Hz respectively); for details of the experimental procedure see the Supplemental Material [20]. In both cases the motion of the low-$k$ superfluid component is visually more clear, and it is more pronounced for the second sound.

We quantitatively analyze these data in two ways. First, in Figs. 3(b) and 3(e), we simply look at the phase $\phi$ of the occupation-number oscillation at each $k$, fitting a sinusoid to $n_k(t) - n_{-k}(t)$ and defining $\phi$ relative to the drive [20]. For second sound, $\phi$ wraps from 0 to $\pi$ with increasing $k$. On the other hand, for first sound, $\phi$ is close to zero for all $k$. Second, we disentangle the motion of normal and superfluid components, which both contribute at low $k$. We deduce $v_n(t)$ by looking only at high $k$ (>1.7 $\mu$m$^{-1}$), assuming that the hydrodynamic motion of the normal component corresponds to a simple displacement of its whole momentum distribution, and then calculate $v_s(t)$ from $v_n(t)$, the total current, and the superfluid fraction [20]. These results are shown in Figs. 3(c) and 3(f). Note that $v_s$ at the first-sound resonance (40 Hz) could be slightly affected by the proximity to the second-sound resonance for $k = 3k_L$.

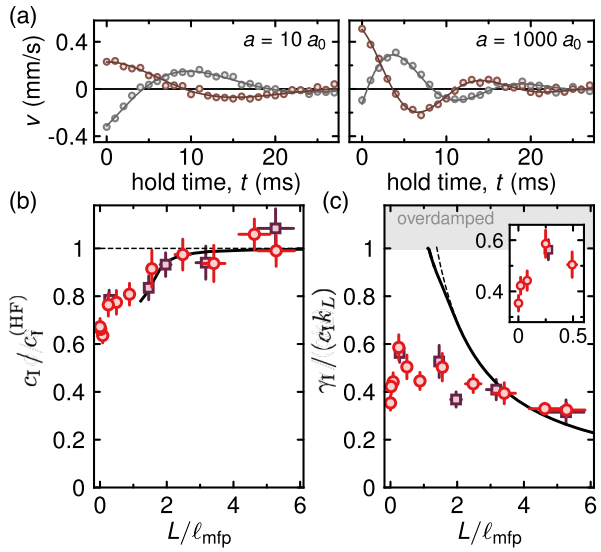


FIG. 4. From collisionless dynamics to hydrodynamic sound in a normal gas. (a) For scattering lengths from $a = 10\ a_0$ to $1000\ a_0$, we measure the COM velocity $v$ for a free oscillation after shaking the cloud for 3 (gray circles) and 3.25 (brown circles) periods at 55 Hz. (b) Measured speed of sound $c_\mathrm{I}$ normalized to the speed $c_\mathrm{I}^{(\mathrm{HF})}$ predicted for dissipationless hydrodynamics. (c) Damping per period. In both (b) and (c), the data for $L = 70\ \mu$m (purple squares) coalesce with the data taken using an additional box geometry ($L = 50\ \mu$m, red circles), when plotted against the inverse Knudsen number $L/\ell_\mathrm{mfp} \sim na^2/k_L$. The dashed lines show theoretical predictions to linear order in $\ell_\mathrm{mfp}/L$, while the solid lines show the results of the full hydrodynamic calculation (see text and the Supplemental Material [20]). The latter captures the observed drop of the normalized sound speed below unity. The relative damping also agrees with this fit-free theory at $L/\ell_\mathrm{mfp} > 3$, while for $L/\ell_\mathrm{mfp} \to 0$ it decreases but remains nonzero (see enlargement in the inset).

These observations demonstrate all the key features of the two-fluid theory for a highly compressible gas. Additional information is contained in the damping of the modes, seen in their nonzero widths [see Fig. 2(b)]; zero hydrodynamic damping would require the collision rate to be infinite, to ensure instantaneous local equilibration, which is not the case even in gases with infinite scattering length [49–51].

For the second sound we deduce an amplitude-damping coefficient $\gamma_\mathrm{II} = 2\pi \times 2.7(4)$ Hz, with no clear $N$ dependence. This is compatible with the Landau–Khalatnikov hydrodynamic prediction [20,52,53] $\gamma_\mathrm{II} \approx 2\pi \times 2.2$ Hz. It also coincides with the Landau-damping prediction [54] $3\pi a k_L k_B T/(8\hbar) = 2\pi \times 2.7(2)$ Hz, but this is likely fortuitous since that theory assumes a collisionless normal component. Note that in the experiment additional broadening may arise due to nonlinear effects [55] and the temporal variation of the gas density caused by losses; in the future it would be interesting to study the damping of the second sound further.

For the first sound, we systematically explore the crossover from the hydrodynamic to the collisionless regime in gases above $T_c$, where hydrodynamic behavior relies entirely on scattering. The parameter separating the two regimes is the Knudsen number, which in our case is given by $\ell_\mathrm{mfp}/L$.

We prepare gases at $T \approx 1.3T_c$ and vary $\ell_\mathrm{mfp}/L$ both by tuning $a$ and using two different box lengths (50 $\mu$m and 70 $\mu$m). We initiate a COM velocity oscillation by shaking at 55 Hz with $F_0 = k_B \times 0.55\ \mathrm{nK}\,\mu\mathrm{m}^{-1}$, then stop the drive and observe decaying free oscillations [see Fig. 4(a)]. We extract the sound speed $c_\mathrm{I}$ and damping $\gamma_\mathrm{I}$ by fitting $v(t)$ with the harmonic-oscillator form $v \propto \cos(\omega_\mathrm{I} t + \phi)e^{-\gamma_\mathrm{I} t}$, with $\omega_\mathrm{I} = \sqrt{(c_\mathrm{I}k_L)^2 - \gamma_\mathrm{I}^2}$. We normalize $c_\mathrm{I}$ by its prediction in the hydrodynamic limit $c_\mathrm{I}^{(\mathrm{HF})}$ [Eq. (2)], and $\gamma_\mathrm{I}$ by the angular frequency $c_\mathrm{I}k_L$.

Theoretically, to linear order in $\ell_\mathrm{mfp}/L$, the sound speed retains its hydrodynamic value, but the nonzero heat conductivity $\kappa$ and viscosity $\eta$ result in a nonzero $\gamma_\mathrm{I}$. The predicted damping, or equivalently the diffusivity $D_\mathrm{I} = 2\gamma_\mathrm{I}/k^2$, is given by the Stokes–Kirchhoff relation $D_\mathrm{SK} = [4\eta/(3mn) + \kappa(c_V^{-1} - c_P^{-1})]$ [56], ignoring the bulk viscosity $\zeta$ in our monatomic gas. In kinetic gas theory $\eta/(mn) \sim \kappa/c_P \sim \ell_\mathrm{mfp} c_\mathrm{I}$. For a weakly interacting gas, $c_\mathrm{I} \sim \sqrt{k_B T/m}$, so $D_\mathrm{I} \sim (\ell_\mathrm{mfp}/\lambda_T)(\hbar/m)$, where $\lambda_T$ is the thermal wavelength, and one can write $\gamma_\mathrm{I}/(c_\mathrm{I}k) = rk\ell_\mathrm{mfp}$, where the dimensionless $r$ depends on the degeneracy; for our $T/T_c$ we get $r \approx 0.44$ [20,57]. This theory, without free parameters, is shown in Figs. 4(b) and 4(c) as the dashed line, and it agrees with our data for $L/\ell_\mathrm{mfp} \gtrsim 3$.

For $L/\ell_\mathrm{mfp} < 3$ the measured $c_\mathrm{I}$ decreases, while $\gamma_\mathrm{I}$ keeps growing albeit less than predicted. Using the classical sound equations, we calculate the effects of $\eta$ and $\kappa$ on $c_\mathrm{I}$ and $\gamma_\mathrm{I}$ beyond linear order (see solid lines in Figs. 4(b) and 4(c), and the Supplemental Material [20,58] for details). The higher-order effects depend on the Prandtl number, Pr, which measures the relative weights of momentum and thermal diffusivities. For our system Pr $\approx 2/3$ [20,57], and the prediction is for $c_\mathrm{I}$ to decrease, in agreement with our data. The predicted damping is also reduced, but not significantly.

In the collisionless regime $L/\ell_\mathrm{mfp} \to 0$, where the hydrodynamic theory does not apply, the measured damping is finite and the oscillations are still well described by an exponential damping. Note that, unlike for the shape oscillations in harmonic traps [8,14], a nonzero damping is expected even at $a = 0$ due to the dispersion of momentum modes.

Finally, we note the distinction between $c_\mathrm{I}$ and the phase velocity $\omega/k$. While $c_\mathrm{I}$ is a material property, the effect of viscous damping on $\omega/k$ depends on the boundary conditions; for our fixed-wavelength case $\omega/k$ decreases with damping, whereas it increases in the fixed-frequency case [20,58].

In conclusion, we observed both first and second sound in a 3D ultracold Bose gas that is sufficiently strongly interacting to be hydrodynamic, but is still highly compressible. We found that Landau's two-fluid theory captures all the essential features of this system, with the first and second sound mode, respectively, predominantly featuring oscillations of the normal and the superfluid component. By tuning interactions, we also studied the breakdown of hydrodynamicity. The experimental access to both microscopic and hydrodynamic properties offers an excellent opportunity for further studies of Bose fluids. In particular, it would be interesting to explore lower temperatures ($k_B T \approx g n_s$) where an avoided crossing of the two sound modes is expected [8]. Below this crossing the incompressible limit is approached and the Bogoliubov mode becomes the first sound, while the nature of the second mode is still a subject of theoretical investigation [59].

The supporting data for this Letter are openly available from [60].

We thank Panagiotis Christodoulou, Ludwig Mathey, Sandro Stringari, and Martin Zwierlein for discussions. This work was supported by EPSRC [Grants No. EP/N011759/1 and No. EP/P009565/1], ERC (QBox), and a QuantERA grant (NAQUAS, EPSRC Grant No. EP/R043396/1). T. A. H. acknowledges support from the EU Marie Skłodowska-Curie program [Grant No. MSCA-IF- 2018 840081]. C. E. acknowledges support from Jesus College (Cambridge). R. P. S. acknowledges support from the Royal Society. Z. H. acknowledges support from the Royal Society Wolfson Fellowship.

*Present address: Max-Planck-Institut für Quantenoptik, 85748 Garching, Germany.
†timon.hilker@mpq.mpg.de

[1] L. Tisza, Transport phenomena in helium II, Nature (London) **141**, 913 (1938).
[2] F. London, The $\lambda$-phenomenon of liquid helium and the Bose–Einstein degeneracy, Nature (London) **141**, 643 (1938).
[3] L. D. Landau, The theory of superfluidity of helium II, J. Phys. USSR **5**, 71 (1941).
[4] L. Landau, Theory of the superfluidity of helium II, Phys. Rev. **60**, 356 (1941).
[5] L. A. Sidorenkov, M. K. Tey, R. Grimm, Y.-H. Hou, L. Pitaevskii, and S. Stringari, Second sound and the superfluid fraction in a Fermi gas with resonant interactions, Nature (London) **498**, 78 (2013).
[6] D. K. Hoffmann, V. P. Singh, T. Paintner, M. Jäger, W. Limmer, L. Mathey, and J. Hecker Denschlag, Second sound in the crossover from the Bose-Einstein condensate to the Bardeen-Cooper-Schrieffer superfluid, Nat. Commun. **12**, 7074 (2021).
[7] M. W. Zwierlein (private communication).
[8] L. Pitaevskii and S. Stringari, *Bose–Einstein Condensation and Superfluidity* (Oxford University Press, Oxford, 2016).
[9] D. S. Jin, J. R. Ensher, M. R. Matthews, C. E. Wieman, and E. A. Cornell, Collective Excitations of a Bose–Einstein Condensate in a Dilute Gas, Phys. Rev. Lett. **77**, 420 (1996).
[10] M.-O. Mewes, M. R. Andrews, N. J. van Druten, D. M. Kurn, D. S. Durfee, C. G. Townsend, and W. Ketterle, Collective Excitations of a Bose–Einstein Condensate in a Magnetic Trap, Phys. Rev. Lett. **77**, 988 (1996).
[11] M. R. Andrews, D. M. Kurn, H.-J. Miesner, D. S. Durfee, C. G. Townsend, S. Inouye, and W. Ketterle, Propagation of Sound in a Bose–Einstein Condensate, Phys. Rev. Lett. **79**, 553 (1997).
[12] D. M. Stamper-Kurn, H.-J. Miesner, S. Inouye, M. R. Andrews, and W. Ketterle, Collisionless and Hydrodynamic Excitations of a Bose–Einstein Condensate, Phys. Rev. Lett. **81**, 500 (1998).
[13] M. Leduc, J. Leonard, F. Pereira dos Santos, E. Jahier, S. Schwartz, and C. Cohen-Tannoudji, Hydrodynamic modes in a trapped gas of metastable helium above the Bose–Einstein transition, Acta Phys. Pol. B **33**, 2213 (2002).
[14] Ch. Buggle, P. Pedri, W. von Klitzing, and J. T. M. Walraven, Shape oscillations in nondegenerate Bose gases: Transition from the collisionless to the hydrodynamic regime, Phys. Rev. A **72**, 043610 (2005).
[15] R. Meppelink, S. B. Koller, and P. van der Straten, Sound propagation in a Bose–Einstein condensate at finite temperatures, Phys. Rev. A **80**, 043605 (2009).
[16] J. L. Ville, R. Saint-Jalm, É. Le Cerf, M. Aidelsburger, S. Nascimbène, J. Dalibard, and J. Beugnon, Sound Propagation in a Uniform Superfluid Two-Dimensional Bose Gas, Phys. Rev. Lett. **121**, 145301 (2018).
[17] A. R. Fritsch, P. E. S. Tavares, F. A. J. Vivanco, G. D. Telles, V. S. Bagnato, and E. A. L. Henn, Thermodynamic measurement of the sound velocity of a Bose gas across the transition to Bose–Einstein condensation, J. Stat. Mech. (2018) 053108.
[18] P. Christodoulou, M. Gałka, N. Dogra, R. Lopes, J. Schmitt, and Z. Hadzibabic, Observation of first and second sound in a BKT superfluid, Nature (London) **594**, 191 (2021).
[19] T. D. Lee and C. N. Yang, Low-temperature behavior of a dilute Bose system of hard spheres. II. Nonequilibrium properties, Phys. Rev. **113**, 1406 (1959).
[20] See Supplemental Material at http://link.aps.org/supplemental/10.1103/PhysRevLett.128.223601, including theory supporting Eqs. (1) and (2), methods used for Fig. 2 and Fig. 3, as well as theory presented in Fig. 4; this also includes the additional Refs. [21–33].
[21] C. J. Pethick and H. Smith, *Bose–Einstein Condensation in Dilute Gases* (Cambridge University Press, Cambridge, England, 2002).
[22] L. Verney, L. Pitaevskii, and S. Stringari, Hybridization of first and second sound in a weakly interacting Bose gas, Europhys. Lett. **111**, 40005 (2015).
[23] F. Gerbier, J. H. Thywissen, S. Richard, M. Hugbart, P. Bouyer, and A. Aspect, Experimental study of the thermodynamics of an interacting trapped Bose-Einstein condensed gas, Phys. Rev. A **70**, 013607 (2004).
[24] R. Lopes, C. Eigen, N. Navon, D. Clément, R. P. Smith, and Z. Hadzibabic, Quantum Depletion of a Homogeneous Bose–Einstein Condensate, Phys. Rev. Lett. **119**, 190404 (2017).

[25] M. Zaccanti, B. Deissler, C. D'Errico, M. Fattori, M. Jona-Lasinio, S. Mueller, G. Roati, M. Inguscio, and G. Modugno, Observation of an Efimov spectrum in an atomic system, Nat. Phys. **5**, 586 (2009).

[26] T. F. Schmidutz, I. Gotlibovych, A. L. Gaunt, R. P. Smith, N. Navon, and Z. Hadzibabic, Quantum Joule–Thomson Effect in a Saturated Homogeneous Bose Gas, Phys. Rev. Lett. **112**, 040403 (2014).

[27] N. Navon, C. Eigen, J. Zhang, R. Lopes, A. L. Gaunt, K. Fujimoto, M. Tsubota, R. P. Smith, and Z. Hadzibabic, Synthetic dissipation and cascade fluxes in a turbulent quantum gas, Science **366**, 382 (2019).

[28] R. P. Smith, N. Tammuz, R. L. D. Campbell, M. Holzmann, and Z. Hadzibabic, Condensed Fraction of an Atomic Bose Gas Induced by Critical Correlations, Phys. Rev. Lett. **107**, 190403 (2011).

[29] S. Pilati, S. Giorgini, and N. Prokof'ev, Critical Temperature of Interacting Bose Gases in Two and Three Dimensions, Phys. Rev. Lett. **100**, 140405 (2008).

[30] I. M. Khalatnikov, *An Introduction to the Theory of Superfluidity* (Addison-Wesley, Redwood City, 1965).

[31] B. Capogrosso-Sansone, S. Giorgini, S. Pilati, L. Pollet, N. Prokof'ev, B. Svistunov, and M. Troyer, The Beliaev technique for a weakly interacting Bose gas, New J. Phys. **12**, 043010 (2010).

[32] N. Prokof'ev, O. Ruebenacker, and B. Svistunov, Weakly interacting Bose gas in the vicinity of the normal-fluid–superfluid transition, Phys. Rev. A **69**, 053625 (2004).

[33] G. Spada, S. Pilati, and S. Giorgini, Thermodynamics of a dilute Bose gas: A path-integral Monte Carlo study, Phys. Rev. A **105**, 013325 (2022).

[34] P. Nozières and D. Pines, *The Theory of Quantum Liquids* (Addison-Wesley, Redwood City, CA, 1990).

[35] The parameter $K^2 = \varepsilon/(1+\varepsilon)$ is directly related to the Landau–Placzek ratio $\varepsilon = c_P/c_V - 1$ [36].

[36] L. Landau and G. Placzek, Structure of the undisplaced scattering line, Phys. Z. Sowjetunion **5**, 172 (1934).

[37] We understand the ideal gas as the limit $a \to 0^+$. The strictly non-interacting gas has $c_{II} = 0$ and is not a superfluid.

[38] A. Griffin and E. Zaremba, First and second sound in a uniform Bose gas, Phys. Rev. A **56**, 4839 (1997).

[39] Generally, in an interacting system, $n_s$ differs from the BEC density $n_{\mathrm{BEC}}$ (see [20]). In Hartree–Fock theory, one finds $n_s = n_{\mathrm{BEC}}$ and so we write Eq. (2) in terms of $n_s$ and $n_n$.

[40] A. L. Gaunt, T. F. Schmidutz, I. Gotlibovych, R. P. Smith, and Z. Hadzibabic, Bose–Einstein Condensation of Atoms in a Uniform Potential, Phys. Rev. Lett. **110**, 200406 (2013).

[41] C. Eigen, A. L. Gaunt, A. Suleymanzade, N. Navon, Z. Hadzibabic, and R. P. Smith, Observation of Weak Collapse in a Bose–Einstein Condensate, Phys. Rev. X **6**, 041058 (2016).

[42] N. Navon, R. P. Smith, and Z. Hadzibabic, Quantum gases in optical boxes, Nat. Phys. **17**, 1334 (2021).

[43] R. J. Fletcher, R. Lopes, J. Man, N. Navon, R. P. Smith, M. W. Zwierlein, and Z. Hadzibabic, Two- and three-body contacts in the unitary Bose gas, Science **355**, 377 (2017).

[44] Throughout the paper, we evaluate $T_c$ based on ideal-gas theory. The expected interaction-induced shift of $T_c$ is on the level of one percent in our system (see [20]).

[45] We checked experimentally that our value of $F_0$ is in the weak-drive regime, such that the positions of the resonances are (within error bars) independent of $F_0$.

[46] N. Navon, A. L. Gaunt, R. P. Smith, and Z. Hadzibabic, Emergence of a turbulent cascade in a quantum gas, Nature (London) **539**, 72 (2016).

[47] R. Anderson, F. Wang, P. Xu, V. Venu, S. Trotzky, F. Chevy, and J. H. Thywissen, Conductivity Spectrum of Ultracold Atoms in an Optical Lattice, Phys. Rev. Lett. **122**, 153602 (2019).

[48] The interaction shift of $c_I$ is noticeable in our system even though the interactions are only just strong enough to reach the hydrodynamic regime. This can be contrasted to air at room temperature, which is very hydrodynamic [$\lambda/\ell_{\mathrm{mfp}} \sim na^2$ $\lambda \approx 10^7$ using $\lambda \approx 1$ m and $\ell_{\mathrm{mfp}} \approx 100$ nm], but almost a perfect ideal gas [$gn/(k_B T) \sim na\lambda_T^2 \approx 10^{-5}$ using an effective $a$ based on $\ell_{\mathrm{mfp}}$] due to the much higher temperature.

[49] P. B. Patel, Z. Yan, B. Mukherjee, R. J. Fletcher, J. Struck, and M. W. Zwierlein, Universal sound diffusion in a strongly interacting Fermi gas, Science **370**, 1222 (2020).

[50] M. Bohlen, L. Sobirey, N. Luick, H. Biss, T. Enss, T. Lompe, and H. Moritz, Sound Propagation and Quantum Limited Damping in a Two-Dimensional Fermi Gas, Phys. Rev. Lett. **124**, 240403 (2020).

[51] X. Wang, X. Li, I. Arakelyan, and J. E. Thomas, Hydrodynamic Relaxation in a Strongly Interacting Fermi Gas, Phys. Rev. Lett. **128**, 090402 (2022).

[52] P. C. Hohenberg and P. C. Martin, Microscopic theory of superfluid helium, Ann. Phys. (N. Y.). **34**, 291 (1965).

[53] T. Nikuni and A. Griffin, Landau–Khalatnikov two-fluid hydrodynamics of a trapped Bose gas, Phys. Rev. A **63**, 033608 (2001).

[54] A. Griffin, T. Nikuni, and E. Zaremba, *Bose-Condensed Gases at Finite Temperatures* (Cambridge University Press, Cambridge, England, 2009).

[55] J. Zhang, C. Eigen, W. Zheng, J. A. P. Glidden, T. A. Hilker, S. J. Garratt, R. Lopes, N. R. Cooper, Z. Hadzibabic, and N. Navon, Many-Body Decay of the Gapped Lowest Excitation of a Bose–Einstein Condensate, Phys. Rev. Lett. **126**, 060402 (2021).

[56] L. D. Landau and E. M. Lifshitz, *Fluid Mechanics* (Elsevier, New York, 1987).

[57] T. Nikuni and A. Griffin, Hydrodynamic damping in trapped Bose gases, J. Low Temp. Phys. **111**, 793 (1998).

[58] S. Temkin, *Elements of Acoustics* (Wiley, New York, 1981).

[59] I. M. H. Seifie, V. P. Singh, and L. Mathey, Squeezed-field path-integral description of second sound in Bose–Einstein condensates, Phys. Rev. A **100**, 013602 (2019).

[60] T. A. Hilker, L. H. Dogra, C. Eigen, J. A. P. Glidden, R. P. Smith, and Z. Hadzibabic, Research data supporting: 'First and Second Sound in a Compressible 3D Bose Fluid', Apollo Repository (2022).